



Investigation of the effect of layered structure on partial discharges in transformer pressboard insulator

Fatih Atalar¹ · N.Özben Önhon² · Mukden Uğur³

Received: 14 August 2022 / Accepted: 14 June 2023 / Published online: 24 June 2023
© The Author(s), under exclusive licence to Springer-Verlag GmbH Germany, part of Springer Nature 2023

Abstract

The dielectric performance of pressboards impregnated with mineral oil is one of the key points in regard to the quality of the transformer's working life. Partial discharges (PDs) occurring in the pressboard can cause some insulation defects which might be one of the major reasons for an electrical breakdown. Detection of the PDs in pressboards gives a chance to understand the dielectric behavior of the insulators, hence major defects can be prevented just in early stage. The main point of the study is to investigate the differences in dielectric performance of layered and non-layered pressboards in the presence of PDs. For this purpose, the PD behavior of a layered pressboard with three layers (each with a thickness of 0.5 mm) and of a non-layered (solid) pressboard (with a thickness of 1.5 mm) is examined for two different high voltage levels (20 and 30 kV). To detect the PDs, Hall Effect Sensors are employed, considering that PDs cause fluctuations in the magnetic field. To analyze the magnetic field measurements from a statistical point of view, the Kaplan–Meier method and the Weibull analysis are used.

Keywords Layered pressboards · Non-layered pressboards · Partial discharge · Kaplan–Meier method · Weibull analysis

1 Introduction

The digital world provides ease of doing business in every sector and allows jobs to be done faster. However, an interruption in electrical energy for any reason, may cause delays and even undesired results in some important services. Therefore, the condition of transformers is crucial for electrical energy systems. Any failure in transformers can cause unpredicted energy cuts. Most of the faults that occur are caused by the loss of the dielectric properties of the insulators under various environmental and electrical stresses. The most commonly used insulators in transformers are mineral oil and pressboard. Pressboards are wrapped between the windings and

these windings are immersed in mineral oil. They significantly increase the dielectric strength of the transformer as they absorb oil [1]. One of the biggest advantages of this material is that it provides mechanical support even at high temperatures. It has a high degree of flexibility, simultaneously possessing high tensile and compression strength.

Like all insulators, pressboards also have a certain lifetime, but during this operational life, regular maintenance can be provided to ensure error-free operation. Cellulose-based bond structure within the solid insulator, which is exposed to a very high electric field, breaks down at the microlevel over time and the charge starts to pass through the insulator [2, 3]. The charge transition continues at the weakest point and perhaps the insulator loses this property by being electrically pierced completely. However, by analyzing the causes of this situation, faults and insulator breakdowns can be prevented.

These papers, which are cellulosic materials, can start to disintegrate as a result of PDs and put the transformer into a fault state. It is extremely important to examine the PD behavior of this paper insulator with such critical importance in the transformer [4]. Partial discharge is one of the most important clues to understand the deterioration process in an insulator. If the PD behavior can be analyzed well, a lot of information about the dielectric behavior of the insulator can

✉ Fatih Atalar
fatih.atarar@iuc.edu.tr

¹ Department of Electrical and Electronics Engineering, Istanbul University-Cerrahpaşa, 34320 Avcılar, Istanbul, Turkey

² Department of Electrical and Electronics Engineering, Turkish-German University, 34820 Beykoz, Istanbul, Turkey

³ Department of Robotics and Intelligent Systems, The Institute of Graduate Studies in Science and Engineering, Turkish-German University, 34820 Beykoz, Istanbul, Turkey

be obtained. Measuring the PD characteristic of an insulator has a very important role in terms of sustainable energy. The paper insulator/pressboard in the transformer can be exposed to high electrical stresses during its operating life and maybe partially discharged. Taking precautions against PDs is as important as measuring the PDs in order to prevent malfunctions [5, 6]. There are many studies in the literature on PD measurement in insulators of transformers and precautions that can be taken against PDs [7–15].

Azrin et al. aged a paper pressboard and a Kenaf/polypropylene pressboard under constant voltage for 6 h separately. They studied surface morphology using PD patterns and a scanning electron microscope (SEM) for both pressboards [7]. They measured that the PD amplitude of the Kenaf/polypropylene pressboard was lower. In addition, in the related study, they revealed that the surface of the classical paper pressboard deteriorates more (the tracks on the surface are larger and deeper) and the dielectric strength is lower.

Chongzhi Zhao et al. measured the PD behavior of the solid insulator in the process up to the breakdown of 50 pressboards in the 24–29 kV range with an increase in 1 kV at each step [8]. They made a statistical evaluation of PD logarithmically using the Gaussian distribution. They computed the distribution of the PD probability by measuring the apparent charge per second, the PD repetition frequency and the phase range width.

Yongqiang Wang et al. exposed the pressboard to high voltage with an increase in 2 kV every 30 s in a hemispherical-plane electrode arrangement. After measuring the PDIV values and critical flashover voltages, the solid insulator surface was analyzed by SEM and FTIR methods. In this way, they tested aged and fresh samples. They used the PD data measuring instrument, which is widely used in experimental studies. In addition, within the scope of their results, they explained that the breakdown voltage of the aged pressboard is low and that the aged pressboard undergoes more deformation in the images obtained from the SEM analysis. [9].

Since the pressboard is a solid insulator, its breakdown resistance is higher than liquids and gaseous. However, if there is a void in this insulator for any reason, the dielectric strength drops significantly. Bing Luo et al. examined the effect of the two-dimensional air gap model of oil-paper insulated pressboard on surface tracking formation and breakdown voltage in pressboards under AC–DC combined voltage [10]. Although their work has a unique direction, they did not examine the layered structure.

Tracking tree formation on the surface due to high electrical stress on the solid insulator surface can significantly reduce the breakdown voltage of the insulator. Yangchun Cheng et al. investigated the carbonized tree type tracking formation on the pressboard surface in the needle-plate electrode configuration [11]. They concluded that white marks

that occurred earlier than tracking gave a very important clue as an easy determination of carbonized tree formation.

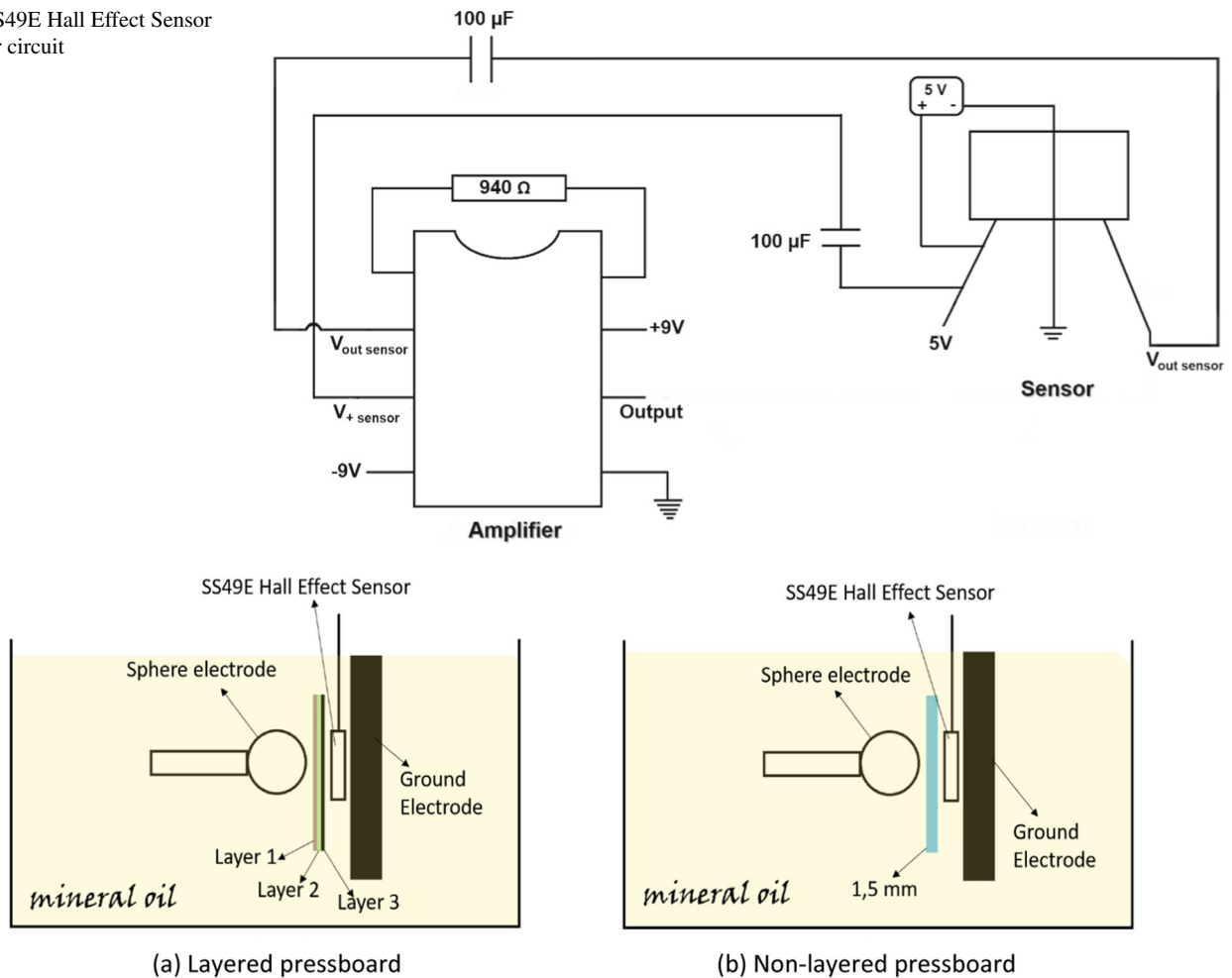
Transformers are also affected by lightning impulse voltages throughout their operational life. Since the lightning impulse voltage reveals a very high electric field in a very short time, the transformer insulators must be well protected against this impulse. K. H. Jang et al. examined the PDs formed at the pressboard–oil interface, adding a thin layer of epoxy resin and Teflon to the surface of the pressboard and compared this two-doped structure with the neat pressboard and dry pressboard [12]. They stated that the epoxy doped insulator has the lowest probability of breakdown, while the dry insulator is the highest. In addition, they concluded that the average discharge length is in the highest undoped insulator.

T. Umemoto et al. tested two pressboards under lightning impulse voltage stress in a rod–plane electrode system with an oil gap (1.6, 2.4, and 3.2 mm) between them [13]. A similar study was carried out by placing a barrier between pressboard and oil under lightning impulse voltage [14]. In both studies, they observed that putting a barrier or oil gap between the pressboard and oil changed the breakdown voltage and PDIV. However, in a real transformer, it is not practical to apply these layouts between the windings. Therefore, other ways of wrapping the pressboard between the windings and creating a layered structure should be sought.

Considering these points, we aim here to compare two different pressboard structures in terms of dielectric strength with an innovative method. With this intention we investigate the PD behavior of a multi layered pressboard wounded on the copper windings and a non-layered pressboard for the voltage levels of 20 and 30 kV. The multi layered pressboard in our experimental setup has three layers each with a thickness of 0,5 mm, and the non-layered pressboard has a thickness of 1,5 mm.

It is known that when an insulator is exposed to high electric field, electrons initiate ionization in transformer oil and pressboard. As ionization gradually increases, electron movements become faster. PD is formed due to this electron movement, which occurs before the complete breakdown of the dielectric material. Since the movement of electrons causes a change in the magnetic field as well, as an alternative method to classical PD measurement, we used Hall Effect Sensors (Honeywell SS49E) for PD detection. The use of Hall Effect Sensor in PD measurement provides advantages in terms of both cost and ease of measurement.

To analyze the magnetic field measurements from a statistical point of view we use a well-known approach, called "Survival Analysis" in the literature. Survival analysis provides statistical information about the occurrence time of an event of interest [16], hence it is used in a broad range of areas such as medicine [17–21], production [22–26], studies of ecology [27–30], economy [31–33], etc. In this work,

Fig. 1 SS49E Hall Effect Sensor amplifier circuit**Fig. 2** Two different structures for pressboard

we handle the PDs as the events of interest. To estimate the occurrence frequency of PDs we apply the nonparametric Kaplan–Meier method [34] and the parametric Weibull method [35, 36]. The analysis results show that the pressboards with a layered structure significantly reduce the occurrence frequency of PDs.

2 Experimental setup

The experimental setup we used in our previous study was also used for the tests of this study in accordance with the same standards [15]. However, in this study, measurements were made using a single op-amp instead of a differential amplifier circuit for the sensor since examining the effect of layered structure on dielectric strength using a single sensor is more important for the experiment. The circuit diagram established for the sensor is shown in Fig. 1.

The sensor has an analog output and this output is amplified with TL081CP DIP-8 OpAmp integrated operational

amplifier. As can be seen in Fig. 1, $100\mu\text{F}$ capacitors are placed at the $+5\text{ V}$ supply and analog output of the sensor. The aim is to suppress noise during the measurement of a PD. The sensor is located between the pressboard insulator and the ground electrode. To obtain the layered structure, after the compression of the layers in a special way, oil impregnation and drying processes were carried out. The pressboard was dried first in a circulating oven at $105\text{ }^\circ\text{C}$ for 48 h and then in a vacuum oven at $85\text{ }^\circ\text{C}$ for 24 h. After drying, oil impregnation was carried out in a vacuum oven at $85\text{ }^\circ\text{C}$ at 5 mbar pressure for 48 h. In this way, any air gap is prevented. In the layered structure, the sensor is placed behind the layer closest to the earth electrode at a clearance of 5 mm. The layered and non-layered structures are shown in Fig. 2.

As it can be seen in Fig. 2a, the layered structure was formed by lining 3 pressboards with 0.5 mm thickness, one after another, without any gaps between them. In Fig. 2b, experiments were carried out using a non-layered pressboard with a thickness of 1.5 mm, equal to the total thickness value

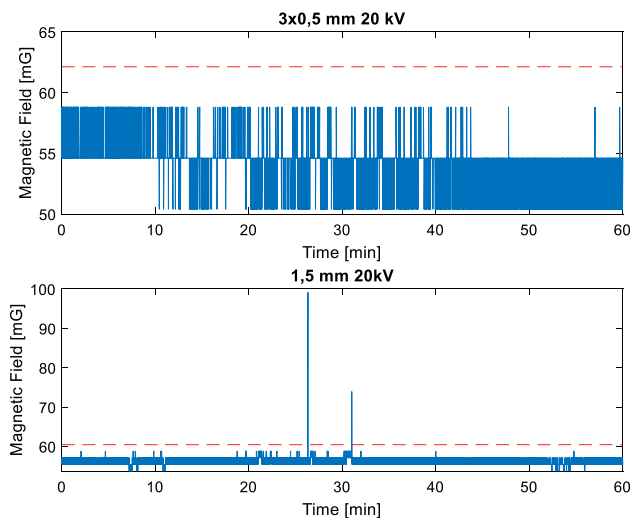


Fig. 3 Magnetic field values of the layered and the non-layered pressboards under 20 kV

of the layered structure. During the experiments, the temperature was kept constant at 23 ± 2 °C and the humidity value at $50\% \pm 10\%$. In the experiments, new transformer oil with a maximum moisture content of 15 ppm was used. Each time the oil was replaced with a new fresh one when the voltage level was changed. The measurements were taken separately for 1 h at 20 kV and 30 kV high voltage values. The voltage value was adjusted with the help of an autotransformer. All experiments were conducted using the same electrode configuration (spherical-plane).

3 Statistical analysis and experimental results

Using the experimental setup explained in the previous section we collected magnetic field measurement results for the layered and non-layered pressboards under 20 and 30 kV voltage values. These measurements are presented in Figs. 3 and 4, respectively.

Since the magnetic field value is expected to increase suddenly during a PD, the points, where the instantaneous peaks arise, give us the potential PD moments. It is seen that all of the signals slightly oscillate around a certain offset value, and only at some peak points do they largely deviate from this offset value. These peaks, which are clearly visible on the graphs, can be automatically found by adaptive thresholding. The procedure used to compute the threshold is given in the block diagram in Fig. 5. To find the threshold value, we first filter the signal with a median filter of length five. The reason for this filtering is to filter out the peak values. After we find the maximum value of the filtered signal which actually corresponds to the maximum value of the oscillating part of the

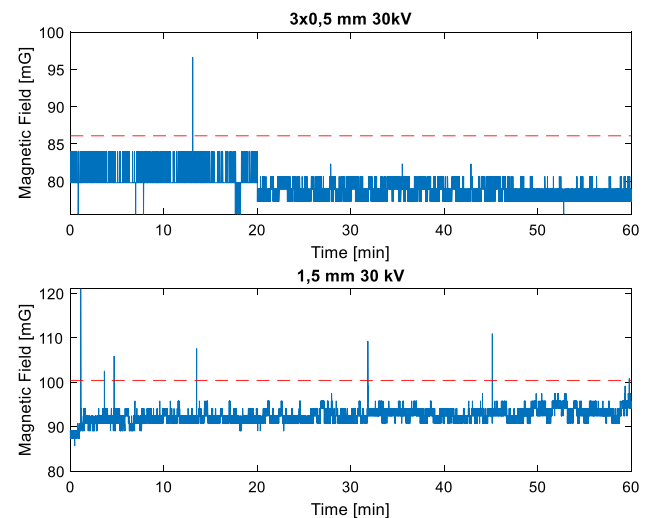


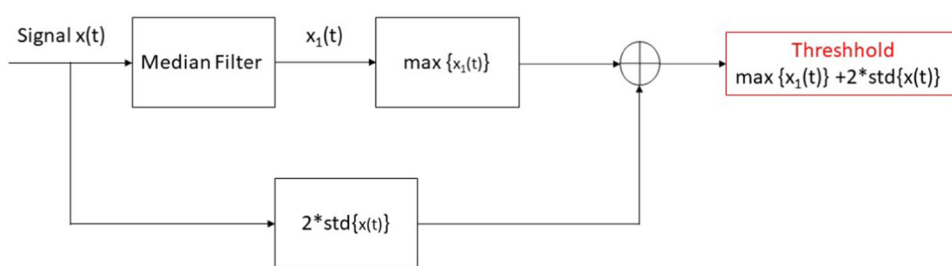
Fig. 4 Magnetic field values of the layered and the non-layered pressboards under 30 kV

signal, we compute the standard deviation of the original signal. We accept the points where the original signal exceeds this maximum value by more than two standard deviations of the signal as potential PD instants. In Figs. 3 and 4, the dashed red line shows the threshold value computed for that signal.

When we examine the signals for the 20 kV voltage, we can say that there is no PD for the layered pressboard, since there is not any peak that exceeds the computed threshold value, while we observe two PDs for the non-layered pressboard. Similarly, when we examine the signals for 30 kV voltage, we can declare only one PD for the layered pressboard, while for the non-layered pressboard there are seven PDs. According to these results, as the applied voltage increases, the frequency of PDs increases. We obtain another important result when we compare the number of PDs for the layered and non-layered pressboards. Although it is much more obvious for 30 kV voltage, under both 20 and 30 kV voltages, the number of PDs for the layered pressboard is fewer than for the non-layered pressboard.

We use a statistical approach to generalize these observations and to analyze the partial discharge behaviors of layered and non-layered pressboards. Survival analysis is a well-known method in the literature that is used to statistically analyze the time of occurrence of a certain event. In all of the survival analysis problems, the outcome variable is the time until an event of interest occurs. The event of interest may vary in a broad range according to the field in which the survival analysis is used. It may be the survival or recovery time of the patients having a specific disease [17–21], the failure time or the lifetime of mechanical or electronic devices and systems [22–26] or even the length of time people remain unemployed after they lost their job [33]. In our

Fig. 5 Block diagram of thresholding procedure



problem, a partial discharge is the event of interest, so the time between the partial discharges can be handled as the "survival time". The survival time is regarded as a random variable, denoted here by T , and the function that gives the probability, the random variable T is greater than a certain time t is defined as the "survival function" $S(t)$ [16]. $S(t)$, as seen in Equation- (1), is actually obtained by subtracting the cumulative distribution function $F(t)$ of the random variable T from 1.

$$S(t) = P(T > t) = 1 - P(T \leq t) = 1 - F(t) \quad (1)$$

Another function used in the analysis, the "hazard function" $h(t)$, indicates the potential that the event occurs at time t , if the event of interest has not occurred until time t . The "cumulative hazard function" $H(t)$ is a rate showing the cumulative sum of the hazard function $h(t)$ up to the time t of interest. $h(t)$ and $H(t)$ are closely related to $S(t)$, and if one is known, it is possible to derive the other. However, both $h(t)$ and $H(t)$ give a rate, not a probability. They are computed as shown in Eq. (2) and Eq. (3) [16].

$$h(t) = \frac{-dS(t)/dt}{S(t)} \quad (2)$$

$$H(t) = \int_0^t h(u)du \quad t > 0 \quad (3)$$

Including the time intervals to the analysis in which the event does not occur during the observation or measurement process is called "censoring," i.e., the survival time for the censored data is not known exactly [16]. In this study, we use the censored data as well.

For statistical analysis, we first use the nonparametric Kaplan–Meier method [34], which creates a probability function using only the measured data. Considering the censored data, the survival function for the Kaplan–Meier method can be formulated as follows:

$$S(t_n) = S(t_{n-1})P(T > t_n | T \geq t_n) \quad (4)$$

If we interpret this formula for the problem in this paper, $S(t_n)$ is the probability of occurring no PD until the time of t_n passes and $S(t_{n-1})$ is the probability of occurring no PD

until the time of t_{n-1} passes. $P(T > t_n | T \geq t_n)$ denotes the conditional probability of a PD after the time of t_n given there is no PD until the time t_n .

Using the Kaplan–Meier method, the PD times for the non-layered pressboard under 30 kV voltage have been analyzed. The results are presented in Table 1. From the graph in Fig. 4, it can be seen that for the non-layered pressboard under 30 kV voltage there are seven peaks in the signal exceeding the threshold value, which we consider as PDs. In the first column of Table 1, the periods between these PDs are given in ascending order. The time interval of 0.2233 min from the last PD to the end of the measurement process is also included in the analysis as censored data.

If we interpret the "survival function" values presented in Table 1, we reach the following conclusions: for the non-layered pressboard under 30 kV voltage, the probability of no occurrence of a partial discharge for approximately 2.5 min long is around 57%, and for approximately 15 min long it is 14%, and the probability of approximately 18 min is 0%. In other words, for this setup approximately every 18 min we can expect at least one partial discharge.

Since the Kaplan–Meier method highly relies on the measured data, the graph of the survival function is not a smooth curve, but rather it is in the form of a step function. In order to generalize our results and to understand how partial discharge times would behave if we had more data, we fit the data to the Weibull distribution, which is frequently used in survival analysis [35, 36]. For the Weibull distribution, the survival function $S(t)$, the hazard function $h(t)$, the cumulative hazard function $H(t)$ and the probability density function $f(t)$ are given in Eqs. (5), (6), (7) and Eq. (8), respectively.

$$S(t) = e^{-(\lambda t)^p} \quad (5)$$

$$h(t) = p\lambda^p t^{p-1} \quad (6)$$

$$H(t) = (\lambda t)^p \quad (7)$$

$$f(t) = p\lambda^p t^{p-1} e^{-(\lambda t)^p} \quad (8)$$

Here, both of the parameters p and λ have positive values. The parameters p and λ are called the shape parameter and the

Table 1 PD frequency analysis with the Kaplan–Meier method

t_n [min] (ordered event times)	e (number of observed events for $t > t_n$)	M (number of events, which occur at time t_n)	C (number of censored events)	$S(t_n)$ (survival function)
0	8	0	0	1
0,2233	8	0	1	1
1,0427	7	1	0	$1*(6/7) = 0,8571$
1,1073	6	1	0	$1*(6/7)*(5/6) = 0,7143$
2,5327	5	1	0	$1*(6/7)*(5/6)*(4/5) = 0,5714$
8,8227	4	1	0	0,4286
13,3113	3	1	0	0,2857
14,6500	2	1	0	0,1429
18,3093	1	1	0	0

scale parameter, respectively. For $p = 1$, the Weibull distribution transforms into an exponential distribution. In order to fit a Weibull distribution to the data, first the parameters p and λ need to be estimated. There are different methods such as the method of moments, maximum likelihood and regression to estimate these parameters. In this paper, the parameters are estimated using the maximum likelihood method. The estimates of the parameters p and λ are found by maximizing the likelihood function for Weibull distribution, as shown in Eq. (9).

$$L(p, \lambda) = \prod_{i=1}^n f(t_i; p, \lambda) = \prod_{i=1}^n p\lambda^p t^{p-1} e^{-(\lambda t_i)^p} \tag{9}$$

The p and λ values, which maximize the likelihood function $L(p, \lambda)$, maximize also the logarithm of the likelihood function $LL(p, \lambda)$ given in Eq. (10). Since it is easier to deal with the $LL(p, \lambda)$ function, the parameters p and λ are found by maximizing $LL(p, \lambda)$.

$$LL(p, \lambda) = \sum_{i=1}^n \ln \left[p\lambda^p t^{p-1} e^{-(\lambda t_i)^p} \right] \tag{10}$$

For the non-layered pressboard under 30 kV voltage, the estimated Weibull distribution parameters are calculated as $p = 1.12358$ and $\lambda = 0.1123$. The corresponding Weibull survival function is displayed in Fig. 6.

As it can be seen in Fig. 6, the Weibull survival function is close to the survival function obtained by the Kaplan–Meier method, which strongly relies on the observed data, as well as it provides a good estimation of how the survival function would look if there would be more data. This result shows that the Weibull distribution is a good choice to analyze and compare the partial discharge behaviors of non-layered and layered pressboards. Therefore, for the rest of the analysis, we use the Weibull method.

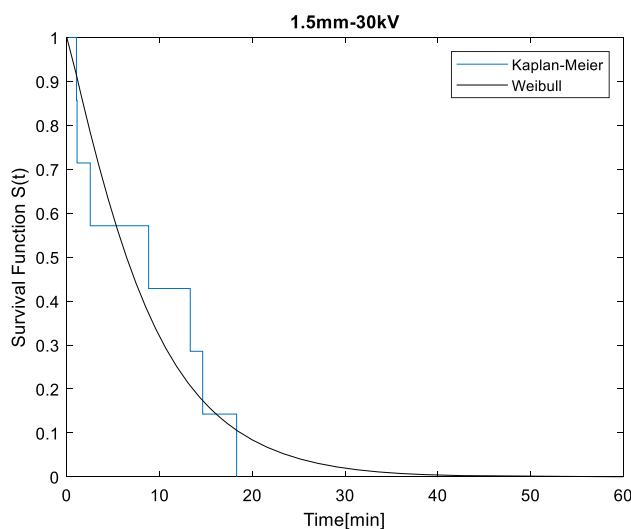


Fig. 6 Survival functions for the non-layered pressboard under 30 kV

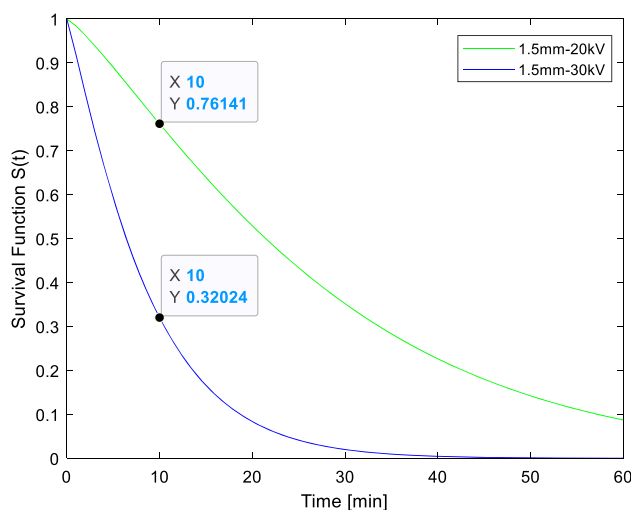


Fig. 7 Weibull survival functions for the non-layered pressboard under 20 and 30 kV

Table 2 Numeric values of Weibull survival functions for the non-layered pressboard under 20 and 30 kV

Time (min)	5	10	15	20	25	30
S(t)-20 kV	0.88979	0.76141	0.63919	0.52926	0.43348	0.3518
S(t)-30 kV	0.59298	0.32024	0.166	0.083657	0.041254	0.019985

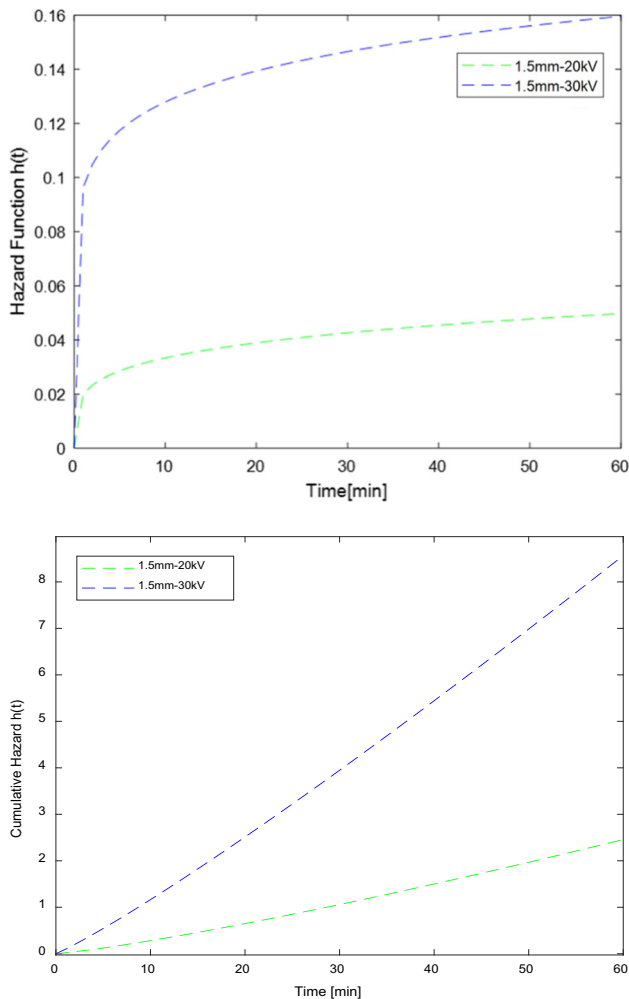


Fig. 8 The hazard function $h(t)$ and the cumulative hazard function $H(t)$ for the non-layered pressboard under the voltage levels 20 and 30 kV

The Weibull survival functions for the non-layered pressboard under 20 and 30 kV voltages are displayed in Fig. 7. Table 2 shows the values of the curves at some sample points. As seen in Table 2, the probability of no occurrence of partial discharge for 5 min long is around 89% for the 20 kV voltage, while it is around 59% for the 30 kV voltage.

Likewise, the probability that a partial discharge will not occur for 30 min is about 35% for 20 kV, while this probability is only about 2% for 30 kV. According to these results, we can conclude that as the applied voltage increases, the periods between PDs shorten, i.e., PDs occur more frequently.

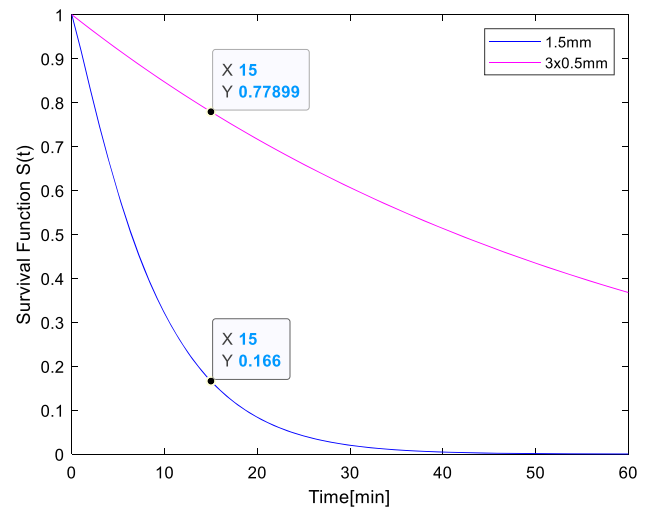


Fig. 9 Survival curves for Weibull distribution under 30 kV

The hazard function $h(t)$ and the cumulative hazard function $H(t)$ displayed in Fig. 8 support these results as well. As the period extends, the potential for a partial discharge increases faster for 30 kV voltage compared to 20 kV voltage.

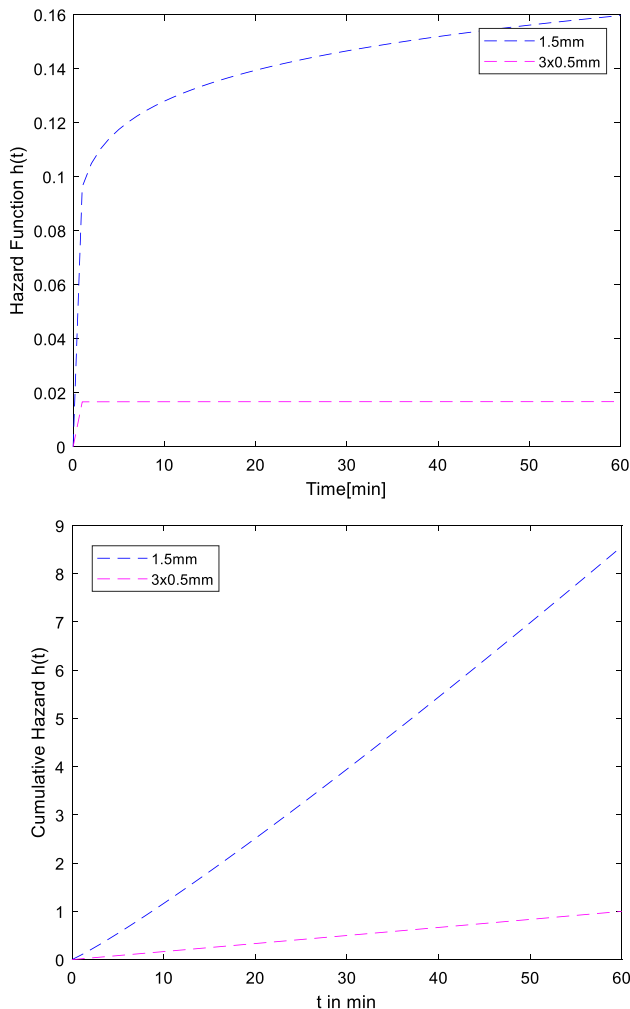
To compare non-layered and layered pressboards under 30 kV voltage we use the survival functions which we obtain through fitting the data to the Weibull distribution. The survival curves and some sampled values from these curves are demonstrated in Fig. 9 and in Table 3, respectively.

As seen in Table 3, the probability of no occurrence of partial discharge for 5 min long is around 92% for the layered pressboard, while this probability is about 59% for the non-layered pressboard. Likewise, the probability that a partial discharge will not occur for 30 min long is approximately 61% for the layered pressboard, while this probability is only about 2% for the non-layered pressboard. Based on these results, we can conclude that a pressboard with a layered structure dramatically reduces the probability of a partial discharge.

The corresponding hazard function $h(t)$ and the cumulative hazard function $H(t)$ displayed in Fig. 10 support these results as well. As the period increases, the potential for partial discharge increases very rapidly for the non-layered pressboard, while it remains almost constant for the layered one.

Table 3 Numeric values of survival curves for Weibull distribution under 30 kV

Time (min)	5	10	15	20	25	30
S(t)-3 × 0.5 mm	0.92021	0.84668	0.77899	0.71668	0.65935	0.60658
S(t)-1.5 mm	0.59298	0.32024	0.166	0.083657	0.041254	0.019985

**Fig. 10** The hazard function $h(t)$ and the cumulative hazard function $H(t)$ for the layered and non-layered pressboards

4 Conclusion

In this paper, we have analyzed the dielectric performance of layered and non-layered pressboards from a quite new perspective. We investigated the magnetic field measurements obtained by Hall Effect Sensors in terms of the PD frequency using a statistical approach called survival analysis. The Kaplan–Meier method and Weibull analysis have been applied to the measured data to extract and generalize the information about the PD characteristics. According to the obtained results, layered and non-layered pressboards

show different dielectric behaviors under high voltage levels. The number of PDs arising in the non-layered structure is higher compared to the one in the layered case. As a result, in our both experimental and statistical analyses, the layered structure shows better dielectric performance than the non-layered one. In order to investigate the dielectric behavior of the layered structure in more detail, further experiments can be performed under different conditions, e.g., different types of electrical stress, lightning impulse, etc.

Acknowledgements This work was supported by the Turkish-German University Research Fund with the Project Code 2019BM0002. The authors would like to thank the Turkish-German University Research Fund for this financial support.

Author's contributions FA contributed to experiments, writing and literature search; ÖÖ contributed to statistical analysis and writing; MU contributed to checking, examine analysis and supervising.

Declarations

Conflict of interest The authors declare no competing interests.

References

- Zhang Y, Qi B, Ma Y, Huang M, Yuan Q, Lv Y, Jiao Y, Li C, Zhang S (2021) Influencing mechanism of adhesive on partial discharge of pressboard block under AC/DC composite voltage. *IEEE Trans Dielectr Electr Insul* 28(6):1883–1891. <https://doi.org/10.1109/TDEI.2021.009610>
- Yoshida S, Kozako M, Hikita M (2021) Characteristics of creepage discharge in oil/pressboard composite insulation. *IEEE Trans Dielectr Electr Insul* 28(2):608–615. <https://doi.org/10.1109/TDEI.2020.009313>
- Zhixian Z, Jiali L, Weigen C, Tianhe Y, Yuxuan S, Kejie W, Fan L (2022) Oil-paper insulation partial discharge ultrasonic multifrequency sensing array based on fibre-optic fabry-perot sensor. *High Voltage* 7(2):325–335. <https://doi.org/10.1049/hve2.12123>
- Li Y, Zhang Q, Ding Y, Zhao Y (2017) Effect of cellulose impurities on partial discharges in oil-pressboard insulation under DC voltage. *IEEE Trans Dielectr Electr Insul* 24(4):2271–2273. <https://doi.org/10.1109/TDEI.2017.006451>
- Li S, Liu Z, Ji S (2021) Characteristics of creeping discharge caused by a needle electrode in oil-pressboard insulation under +DC voltage. *IEEE Trans Dielectr Electr Insul* 28(1):215–222. <https://doi.org/10.1109/TDEI.2020.009157>
- Zhang R, Zhang Q, Guo C, Zhang Z, Wu Z, Wen T (2022) Effects of thermally induced bubbles on the discharge characteristics of oil-impregnated pressboard. *IEEE Trans Dielectrics Electrical Insul*. Early Access. <https://doi.org/10.1109/TDEI.2022.3165737>
- Azrin NA, Ahmad MH, Piah MAM, Talib MA, Nawawi Z (2017) Partial discharge characteristics of oil-impregnated Kenaf based

- pressboard. In: The IEEE student conference on research and development (SCOREd), pp 13–14 Dec 2017, Putrajaya, Malaysia, pp 366–370
8. Zhao C, Song Y, Cheng Y, Xue Y (2016) Risk assessment of oil impregnated pressboards using the statistical distribution of partial discharge before breakdown. In: IEEE international conference on dielectrics (ICD), 3–7 July 2016. University of Montpellier, France, pp 654–657
 9. Wang Y, Zhang X, Jiang X, Wang Y (2019) Effect of aging on material properties and partial discharge characteristics of insulating pressboard. *BioResources* 14(1):1303–1316
 10. Bing L, Jian W.g, Dong D., Lei J., Licheng L. and Tingting W. (2021) Partial discharge simulation of air gap defects in oil-paper insulation paperboard of converter transformer under different ratios of AC–DC combined voltage. *Energies* 14(21):6995. <https://doi.org/10.3390/en14216995>
 11. Yangchun C, Jinqing W, Chongzhi Z, Haoyong S (2016) Experimental research on creepage discharge between oil-impregnated pressboard layers. In: IEEE conference on electrical insulation and dielectric phenomena (CEIDP), Toronto, ON, Canada, pp 999–1002
 12. Jang KH, Yoshida S, Kozako M, Hikita M (2015) Effect of thin solid layer coating on creepage discharge characteristics in oil/pressboard composite insulation system. In: IEEE conference on electrical insulation and dielectric phenomena (CEIDP), Ann Arbor, MI, USA, pp 832–835
 13. Umemoto T, Kainaga S, Muto Tsurimoto H, Yoshida T, Kozako SM, Hikita M (2014) Characteristics of partial discharge in the oil gap separated by pressboard barrier in oil/pressboard composite insulation system. In: IEEE 18th international conference on dielectric liquids (ICDL), Bled, Slovenia, pp 1–4
 14. Yoshida S, Kozako M, Hikita M, Umemoto T, Kainaga S, Muto H, Tsurimoto T (2014) Characteristics of discharge generation across insulation barrier in the oil/pressboard composite insulation system. In: Proceedings of 2014 international symposium on electrical insulating materials, Niigata, Japan, pp 225–228
 15. Atalar F, Uzunoğlu CP, Cekli S, Ugur M (2020) Statistical analysis of induced magnetic fields on oil-impregnated insulation pressboards. *Electr Eng* 102:2095–2107. <https://doi.org/10.1007/s00202-020-01012-8>
 16. Kleinbaum DG, Klein M (2011) *Survival Analysis, a self-learning text, Third Edition*, Springer, ISBN 978–1–4419–6646–9
 17. Mishiro Y, Sakagami M, Kitahara T, Kondoh K, Okumura S (2008) The investigation of the recurrence rate of cholesteatoma using kaplan-meier survival analysis. *Otol Neurotol* 29(6):803–806. <https://doi.org/10.1097/MAO.0b013e318181337f>
 18. Sanders DS, Carter MJ, D’Silva J, James G, Bolton RP, Bardhan KD (2000) Survival analysis in percutaneous endoscopic gastrostomy feeding: a worse outcome in patients with dementia. *Am J Gastroenterol* 95(6):1472–1475. [https://doi.org/10.1016/S0002-9270\(00\)00871-6](https://doi.org/10.1016/S0002-9270(00)00871-6)
 19. Bartel AFP, Thomas SR (2015) Total ankle replacement survival rates based on kaplan-meier survival analysis of national joint registry data. *Clin Podiat Med Surg* 32(4):483–494. <https://doi.org/10.1016/j.cpm.2015.06.012>
 20. Chuang SK, Tian L, Wei LJ, Dodson TB (2001) Kaplan-Meier analysis of dental implant survival: a strategy for estimating survival with clustered observations. *J Dent Res* 80(11):2016–2020. <https://doi.org/10.1177/00220345010800111301>
 21. Zhu HP, Xia X, Yu CH (2011) Application of weibull model for survival of patients with gastric cancer. *BMC Gastroenterol* 11:1. <https://doi.org/10.1186/1471-230X-11-1>
 22. Jean-Francois C, Saleh JH (2009) *Satellite and satellite subsystems reliability: statistical data analysis and modeling*. Elsevier Reliab Eng Syst Safety 94(11):1718–1728. <https://doi.org/10.1016/j.res.2009.05.004>
 23. Jardine AKS, Anderson PM, Mann DS (1987) Application of the weibull proportional hazards model to aircraft and marine engine failure data. *Wiley Quality Reliable Eng Int* 3(2):77–82. <https://doi.org/10.1002/qre.4680030204>
 24. Djamel D, Bachir R (2020) Weibull analysis of fatigue test in jute reinforced polyester composite material, *composites communications* 17:pp123–128. ISSN 2452–2139. <https://doi.org/10.1016/j.coco.2019.11.016>.
 25. Zhai LY, Lu WF, Liu Y, Li X, Vachtsevanos G (2013) Analysis of time-to-failure data with weibull model in product life cycle management. In: Nee A, Song B, Ong SK (eds) *Re-engineering manufacturing for sustainability*. Springer, Singapore. https://doi.org/10.1007/978-981-4451-48-2_114.
 26. Qing Z, Cheng H, Guanghua X (2014) A Mixture weibull proportional hazard model for mechanical system failure prediction utilising lifetime and monitoring data. *Mech Syst Signal Process*. 43(1–2):103–112. ISSN 0888–3270. <https://doi.org/10.1016/j.ymsp.2013.10.013>.
 27. Gayle M (1987) Ecological use of failure time analysis. *Ecol Soc Am* 67(1). <https://doi.org/10.2307/1938524>
 28. David AP, John NT (1986) Statistical analysis of survival and removal rate experiments. *Ecol Soc Am* 67(1). <https://doi.org/10.2307/1938523>.
 29. Caesar AJ (2003) Synergistic interaction of soilborne plant pathogens and root-attacking insects in classical biological control of an exotic rangeland weed. *Biol Control* 28(3):144–153
 30. Michael CN, Michael SA (1992) Enhancing toxicity data interpretation and prediction of ecological risk with survival time modeling: an illustration using sodium chloride toxicity to mosquitofish (*Gambusia Holbrooki*). *Aquatic Toxicol* 23(2):85–96. [https://doi.org/10.1016/0166-445X\(92\)90001-4](https://doi.org/10.1016/0166-445X(92)90001-4)
 31. Ishak KJ, Kreif N, Benedict A, Noemi M (2013) Overview of parametric survival analysis for health-economic applications. *Pharmacoeconomics* 31:663–675. <https://doi.org/10.1007/s40273-013-0064-3>
 32. Evrensel AY (2008) Banking crisis and financial structure: a survival-time analysis. *Int Rev Econ Finance* 17(4):589–602. <https://doi.org/10.1016/j.iref.2007.07.002>
 33. Meyer BD (1990) Unemployment insurance and unemployment spells. *Econometrica* 58(4):757–782. <https://doi.org/10.2307/2938349>
 34. Kaplan EL, Meier P (1958) Nonparametric estimation from incomplete observations. *J Am Stat Assoc* 53(282):457–481
 35. Govind SM, Deo KS, Georgia DK (1996) A generalization of the weibull distribution with application to the analysis of survival data. *J Am Stat Assoc* 91(436):1575–1583. <https://doi.org/10.1080/01621459.1996.10476725>
 36. Kevin JC (2003) On the use and utility of the weibull model in the analysis of survival data. *Controlled Clin Trials* 24(6):682–701. [https://doi.org/10.1016/S0197-2456\(03\)00072-2](https://doi.org/10.1016/S0197-2456(03)00072-2)

Publisher’s Note Springer Nature remains neutral with regard to jurisdictional claims in published maps and institutional affiliations.

Springer Nature or its licensor (e.g. a society or other partner) holds exclusive rights to this article under a publishing agreement with the author(s) or other rightsholder(s); author self-archiving of the accepted manuscript version of this article is solely governed by the terms of such publishing agreement and applicable law.